Title No. 57-68

Camber in Prestressed Concrete Beams

By D. E. BRANSON and A. M. OZELL

Investigation examined experimentally the initial-plus-time-dependent camber deformation in both noncomposite and composite prestressed concrete beams. Methods for calculating these deformations relative to certain properties of the concrete are presented. Ten noncomposite beams and five composite beams were used in the tests. Total camber deformation was found to follow closely the prestress level (relative to concrete strength) but to be relatively insensitive to different concrete strengths and atmospheric conditions. Total camber appears to reach its ultimate value relatively early (100 to 200 days for the test beams) compared to the long-time shrinkage and creep strains that occur. The analytical methods set forth for predicting camber deformation in both noncomposite and composite beams were found to be in good agreement with the test results. The necessary concrete coefficients for the analysis of total camber were experimentally determined and are presented here and recommended for design purposes.

■ IN PRACTICE IT HAS BEEN FOUND that initial camber generally exceeds the expected or computed camber when the latter is based on the cylinder modulus of elasticity. One of the main reasons for this is that the elastic and creep strains occur together during the stressing operation and it is virtually impossible, from a practical standpoint, to obtain a purely elastic or initial camber. Also, the rate of concrete creep is rapid immediately following prestressing, so that the camber does not just occur initially and stop, but is rather a progressive behavior from the start.

Generally speaking, ultimate values of the ratio of creep strain to elastic strain (C_u) of 1.0, 2.0, and 3.0 correspond to relative humidities of approximately 100, 70, and 50 percent, respectively. The ACI-ASCE Committee Recommendations[1] provide for general time-dependent camber calculations by allowing the concrete strains to increase ultimately from 100 to 300 percent ($C_u = 1.0$ to 3.0), depending on atmospheric conditions. This is seen to be the general approach to the problem without specific provision for the effect of different stress levels, prestress loss, increase in concrete stiffness with age, differential shrinkage, and additional slab resistance to camber growth for composite beams.

Even if the creep coefficient C (ratio of creep strain to elastic strain) under constant uniform sustained stress is known, the stress distribution is nonuniform and the sustained stress magnitude varies because of the loss of prestress. This paper includes a study of these and other factors that influence the initial-plus-time-dependent camber deformation in both noncomposite and composite beams.

Notation

1 = subscript denoting the cast-in-place slab of a composite beam

2 = subscript denoting the precast stem of a composite beam

3 = area

B = camber coefficient defined as the ratio of inelastic camber to elastic camber

C = creep coefficient defined as the ratio of creep strain to elastic strain

C_v = creep coefficient for the variable sustained stress in a prestressed concrete beam

c = distance from the centroid of the area of a beam cross section to the extreme fiber

c = subscript denoting concrete

d = depth of a beam cross section

E = modulus of elasticity

E_{sus} = reduced or sustained modulus defined as the ratio of concrete stress to elastic-plus-creep strain

e = eccentricity (e_o at beam end and e_m at midspan)

ε = unit strain

F = differential shrinkage force

f_c' = concrete strength at 28 days

f'_{ci} = concrete strength at the time of prestressing (for the experimental work included herein, all prestressing was done at 28 days)

H = slope of strain distribution diagram

I = moment of inertia (second moment of the area)

i = subscript denoting an initial value

k = prestress loss coefficient defined as the ratio $(P_i - P_t)/P_i$

L = beam span (c-c of supports)

M = bending moment

M' = bending moment resulting from slab dead load

P = prestress force

p = subscript denoting the time of prestressing

q = subscript denoting the time of slab casting

R = radius of curvature

θ = rotation

S = summation coefficient defined by Eq. (6)

σ = unit stress

t = subscript denoting variable time measured from time of prestressing

t' = subscript denoting variable time measured from time of slab casting

u = subscript denoting the time beyond which there is negligible change; i.e., the ultimate value

w = uniformly distributed load

w' = uniformly distributed slab dead load

X = measured camber

x = variable distance along a beam

Y = computed camber using the summation coefficient S_t

y = variable deflection of a beam

Z = computed camber using the slope of the measured strain distribution diagram

$B'_{t'}$, $C'_{vt'}$, $S'_{t'}$ = notation referring to the increase in the respective coefficients for time t' (following slab casting), but where the sustained stress was applied at the time of prestressing

ACI member **D. E. Branson** is associate professor of civil engineering, University of Alabama, Auburn. Dr. Branson was engaged in prestressed concrete research from 1958 to 1960 at the University of Florida where he obtained his PhD in 1960. Portions of his thesis are included in this paper. He is a member of ACI Committee 335, Deflection of Concrete Building Structures.

ACI member **A. M. Ozell**, Professor of Civil Engineering, University of Florida, Gainesville, has been engaged in prestressed concrete research for the past 6 years. Dr. Ozell has written numerous papers, many of them appearing in the ACI JOURNAL, reporting the results of his static and fatigue tests, and other research activities.

DESCRIPTION OF SPECIMENS AND TEST DATA

This study was conducted on five pairs of beams. Each pair consisted of one composite beam and one bare beam. Shrinkage specimens and control cylinders were used for each type of concrete. Table 1 is a summary of information for the beams.

All ten beams were post-tensioned at 28 days with three straight unbonded ¾ in. steel bars. The beam dimensions were 8 in. x 12 in. x 20 ft, and the slabs were 3 in. x 26 in. x 20 ft, as shown in Fig. 1. The steel bars had a modulus of elasticity of 26.38×10^6 psi and a yield strength (0.2 percent offset) of 147,000 psi.

A mechanical strain gage (10 in. gage length) was used to measure the concrete strains. The gage points were steel inserts imbedded in the concrete. Each beam had four gages distributed from top to bottom (see Fig. 1) at both ends and midspan on both sides. Thus a total of 24 gages on each beam provided the data for determining the shrinkage and creep strains in the beams. Dial gages were used on both sides of each beam at midspan to measure the total camber deformation. An average of the two readings is reported for each beam. The accuracy of the dial gages (0.001 in.) for measuring total camber values of up to 1 in. and higher provided excellent data for this part of the study. Camber measurements for the composite beams at midspan were obtained using a Dumpy level and scale providing readings to 0.002 in. Additional data obtained included temperature and relative humidity and the strength and elastic properties of the concrete as determined by 6 x 12 in. cylinder tests.

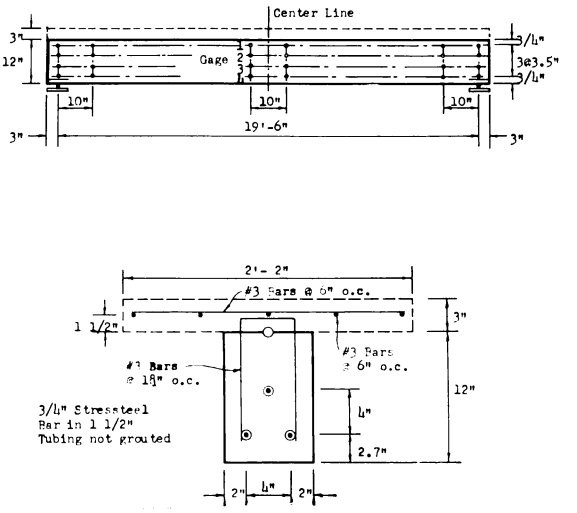

Fig. 1 — Bare beam with cast-in-place slab shown dotted

TABLE 1 — BEAM DATA

Beam No.	Concrete strength 28 days, psi	Stress, percent f'_{ci}	Level, psi	Location	Composite beam No.	Time between prestressing and slab casting, days
1,2	5030	25	1250	Lab	1-C	101
3,4	5030	45	2250	Lab	4-C	101
5,6	5030	65	3250	Lab	6-C	101
7,8	3760	60	2250	Lab	8-C	37
9,10	3760	60	2250	Field	10-C	93

A summary of the test beam data is given in Table 2. Fig. 2 and 3 show some of the specimens and laboratory testing site. The shrinkage data for the beams are shown in Fig. 4. Typical curves showing the elastic-plus-creep strains (for Beam 4) at four gage levels (for both the beam end and midspan sections) are presented in Fig. 5, and the corresponding strain distribution diagrams are shown in Fig. 6. The total midspan camber versus time curves for the ten beams are shown in Fig. 7.

CAMBER OF NONCOMPOSITE BEAMS

The initial curvature expression for any prestressed concrete beam (symmetrical or unsymmetrical with respect to the horizontal centroidal axis) under the action of the beam dead load and the prestress force is given by

$$\frac{d^2y}{dx^2} = \frac{1}{E_p I}(M_x - P_i e_x) \quad \text{.....(1)}$$

where E_p is Young's modulus at the time of prestressing, and P_i is the initial prestress force. For ranges of working stress in the type of concrete ordinarily used for prestressed concrete, the idealized stress-strain curve shown in Fig. 8 for an instantaneous and then constant sustained stress is closely realized. It follows that for a constant sus-

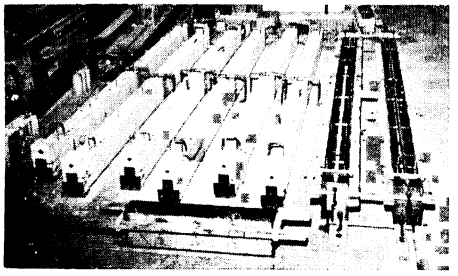

Fig. 2—Laboratory site showing Beams 1-6, shrinkage specimens, dial gage frames, and forms for Beams 7 and 8

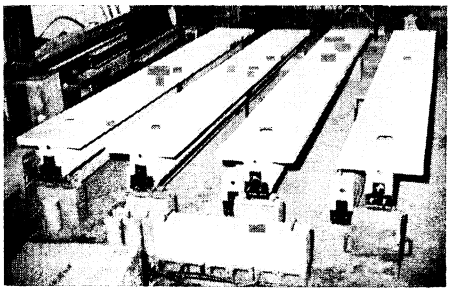

Fig. 3 — Four composite beams in laboratory with noncomposite beams alongside

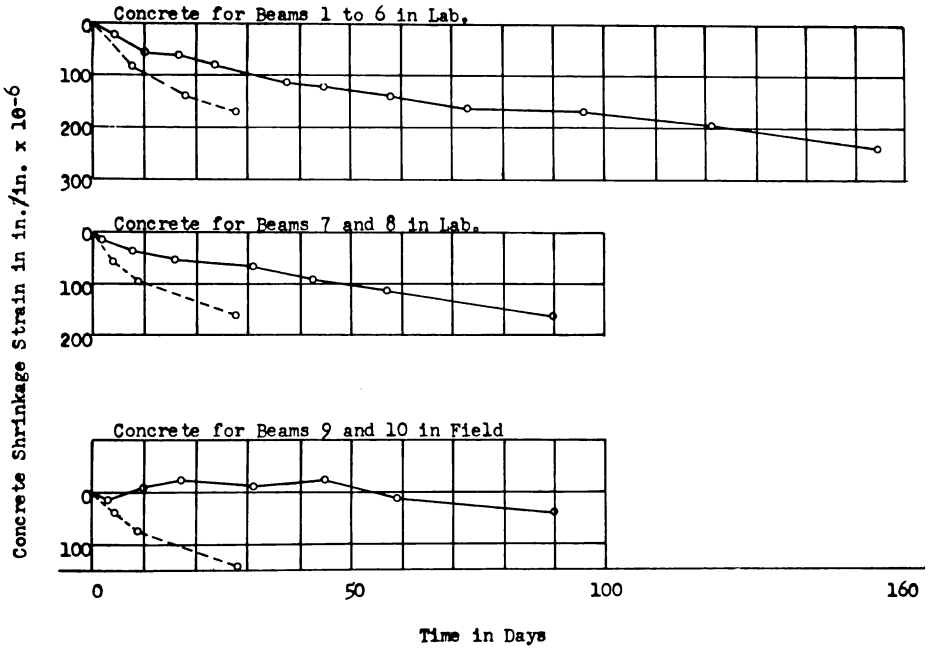

Fig. 4—Concrete shrinkage versus time for precast beam concretes. Each plotted point is an average of 16 readings which indicated a uniform shrinkage strain distribution for the size members used. The dotted curves show the concrete shrinkage from the casting day up to 28 days. Time zero is 28 days after casting at which time the prestress was applied

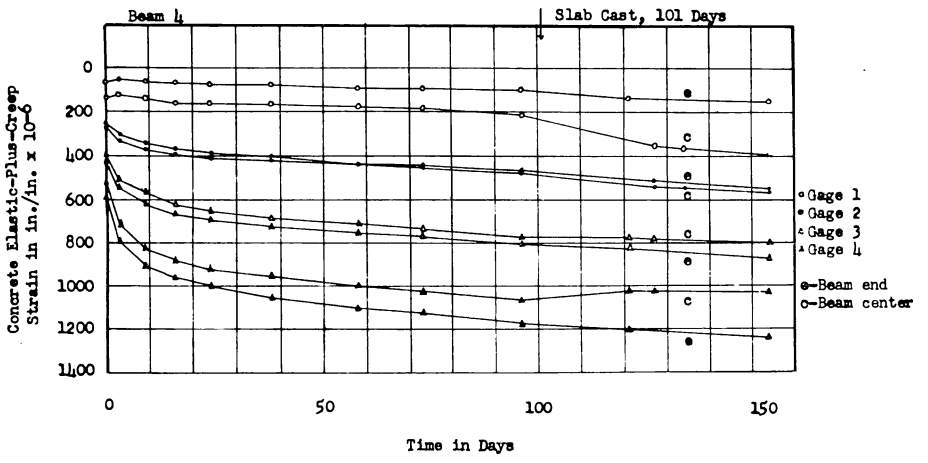

Fig. 5—Concrete elastic-plus-creep strains (Beam 4). Ultimate shrinkage distribution: 9 days—5, 31 days—99, 90 days—167, 154 days—237 in. per in. x 10^{-6}

TABLE 2 — SUMMARY OF DATA FOR THE TEN PRESTRESSED CONCRETE BEAMS

Beam No.	Bar No. (1 • 2 3 • •)	Jack load, kips	Actual load using electrical gages,* kips	Actual total load P, kips	Measured eccentricity at beam end e_o, in.	Actual eccentricity at midspan e_m, in.	Total Pe_o, in.-kips	Total Pe_m, in.-kips	Actual eccentricity of center of gravity of section $e = Pe/P$†		Initial computed stresses				σ_{max}‡ percent f'_{ci}
											End		Midspan		
									End, in.	Midspan, in.	σ_T, psi	σ_B, psi	σ_T, psi	σ_B, psi	
1	1	21	18.6	57.9	−0.56	−0.41	125.0	133.5	2.16	2.31	+ 28	−1352	−250	−1059	26.9
	2	21	19.8		3.41	3.56									
	3	21	19.5		3.48	3.62									
2	1	21	22.1	65.1	−0.62	−0.47	131.6	140.9	2.02	2.16	− 17	−1470	−291	−1182	29.2
	2	21	20.8		3.38	3.52									
	3	21	22.2		3.38	3.52									
3	1	36	33.2	101.5	−0.49	−0.25	223.4	247.8	2.20	2.44	+ 73	−2394	−119	−2190	47.5
	2	36	33.0		3.51	3.75									
	3	36	35.3		3.51	3.75									
4	1	36	37.2	99.9	−0.60	−0.25	190.6	225.9	1.91	2.26	− 86	−2190	−219	−2048	43.6
	2	36	31.0		3.38	3.75									
	3	36	31.7		3.41	3.75									
5	1	50	49.7	142.1	−0.60	−0.25	283.8	334.1	2.00	2.35	− 55	−3188	−106	−3130	63.5
	2	50	47.7		3.38	3.75									
	3	50	44.7		3.41	3.75									
6	1	50	46.7	139.5	−0.65	−0.25	283.3	336.4	2.03	2.41	− 28	−3156	− 64	−3112	63.8
	2	50	46.6		3.41	3.75									
	3	50	46.2		3.35	3.75									
7	1	36	35.7	93.6	−0.51	−0.25	184.5	208.2	1.97	2.22	− 48	−2083	−242	−1875	55.4
	2	36	29.2		3.52	3.75									
	3	36	28.7		3.48	3.75									
8	1	36	26.2	87.4	−0.51	−0.25	200.6	222.9	2.30	2.55	+108	−2106	− 95	−1891	56.0
	2	36	28.7		3.48	3.75									
	3	36	32.5		3.51	3.75									

9	1	36	30.1	90.0	−0.34	−0.25	209.8	217.5	2.33	2.41	+129	−2187	−154	−1890	58.3
	2	36	30.0		3.70	3.75									
	3	36	29.9		3.63	3.75									
10	1	36	28.5	91.6	−0.28	−0.25	220.6	229.6	2.41	2.51	+170	−2265	−106	−1975	60.4
	2	36	30.2		3.54	3.75									
	3	36	32.9		3.70	3.75									

*These values were used in the calculations.
†The midspan eccentricity is greater than at the beam end because of camber.
‡The 28-day cylinder strengths were 5030 psi for Beams 1-6 and 3760 psi for Beams 7-10. The beams were prestressed at 28 days.

tained prestress force, the curvature expression after any time t would be given by

$$\frac{d^2y}{dx^2} = \frac{1 + C_t}{E_p I}(M_x - P_i e_x) \quad \text{.....(2)}$$

where C_t is the creep coefficient corresponding to the time t.

Now consider the effect of the variable sustained stress resulting from the loss of prestress and introduce the prestress loss coefficient $k_t = (P_i - P_t)/P_i$.

This is an important consideration since the initial prestress force is usually reduced from 15 to 30 percent. Eq. (2) is now written as

$$\frac{d^2y}{dx^2} = \frac{1 + C_{v_t}}{E_p I}(M_x) - \frac{1}{E_p I}(P_i e_x) + \left[\sum_{n=0}^{t} \frac{k_n - k_{n-1}}{E_n}\right](P_i e_x)\frac{1}{I} - \left[\sum_{n=0}^{t}(1 - k_n)(C_{v_n} - C_{v_{n-1}})\right](P_i e_x)\frac{1}{E_p I} \quad \text{.....(3)}$$

where C_{v_t} is the creep coefficient for the variable sustained stress for any time t and n is any feasible increment of time. The first term is the elastic-plus-inelastic curvature expression for the dead load moment M_x. This bending moment does not vary with time. The second term is the elastic curvature expression for the initial prestress force. The third term is the curvature expression for the elastic deflection resulting from the loss of prestress $k_n P_i$. It is necessary to express this in a form requiring the summation of the incremental values of k_n/E_n since the history of the stress loss factor k_t and the concrete stiffness E_t must be taken into account. The last term is the curvature expression for the inelastic camber deformation involving the actual prestress force $(1 - k_n)P_i$ and the effective creep coefficient ΔC_{v_t} during the increment of time. The history of the actual prestress force and creep coefficient under variable sustained stress is thus taken into account.

Notice that, in the first and last terms which contain the actual creep coefficient

under the variable stress, Young's modulus at the time of prestressing is used. The reason for this is that the actual experimentally determined creep coefficient would include any inelastic effect of the concrete increasing in stiffness with time.

Eq. (3) can be rewritten in the form

$$\frac{d^2y}{dx^2} = \frac{1}{E_p I}\left[(1 + C_{v_t}) (M_x) \right] + \frac{1}{E_p I}\left[-1 + \sum_{n=0}^{t} \frac{k_n - k_{n-1}}{E_n/E_p} - \sum_{n=0}^{t} (1 - k_n) (C_{v_n} - C_{v_{n-1}}) \right](P_i e_x) \quad \text{.....(4)}$$

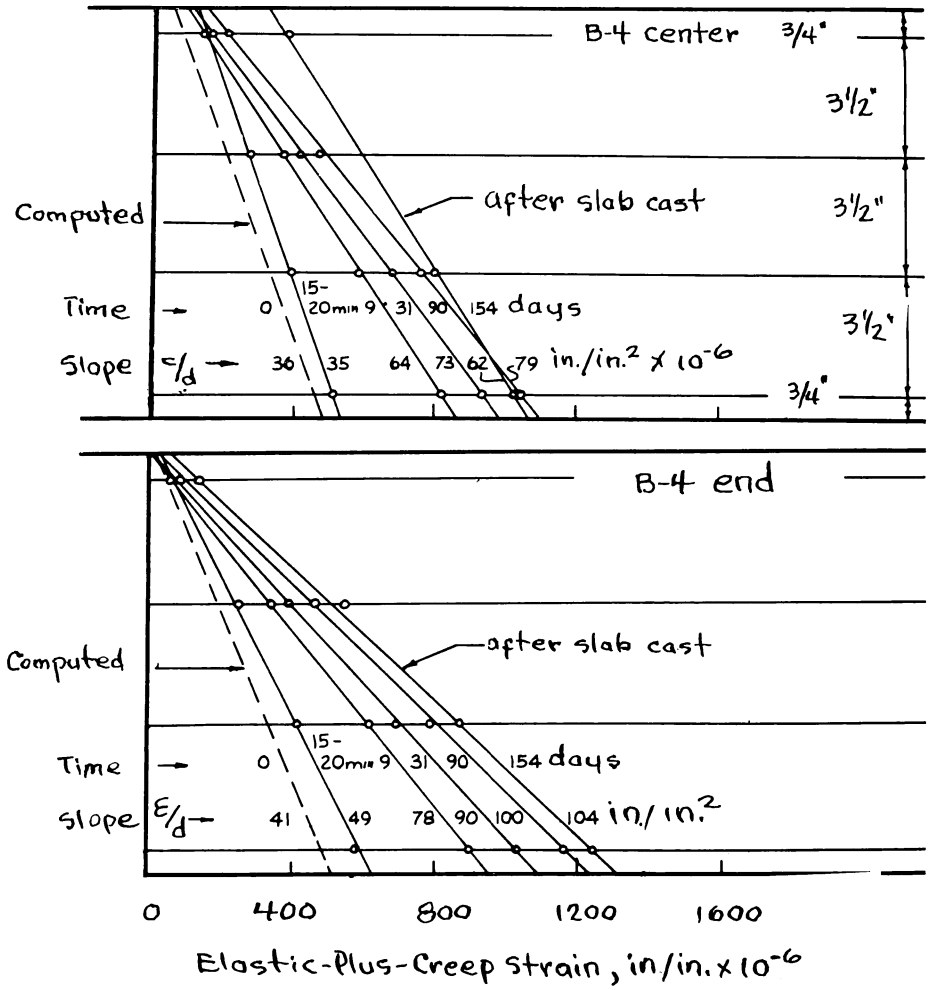

Fig. 6—Elastic-plus-creep-strain distribution diagrams (Beam 4)

which reduces to Eq. (2) when the prestress loss is zero. For convenience Eq. (4) is written as

$$\frac{d^2y}{dx^2} = \frac{1}{E_p I}\left[(1 + C_{v_t}) (M_x) - (1 + S_t) (P_i e_x) \right] \quad \text{.....(5)}$$

where

$$S_t = -\sum_{n=0}^{t} \frac{k_n - k_{n-1}}{E_n/E_p} + \sum_{n=0}^{t} (1 - k_n) (C_{v_n} - C_{v_{n-1}}) \quad \text{.....(6)}$$

The coefficient S_t will be referred to as the summation coefficient.

The solution of Eq. (5) for midspan camber of simply supported prestressed concrete beams is given by the following two equations: For a straight cable

$$y = \frac{1}{E_p I}\left[(1 + S_t) P_i L^2 e/8 - (1 + C_{v_t}) 5wL^4/384 \right] \quad \text{.....(7)}$$

For a parabolic cable

$$y = \frac{1}{E_p I}\left[(1 + S_t) \frac{P_i L^2}{48} (e_o + 5e_m) - (1 + C_{v_t}) 5wL^4/384 \right] \quad \text{.....(8)}$$

It is seen that the summation coefficient S_t corresponds to a creep coefficient but would always be somewhat smaller. This can best be shown by referring to Eq. (6). The factor $(C_{v_n} - C_{v_{n-1}})$ is equal to C_{v_t} for any time $n = t$, and the factor $(1 - k_t)$ is always less than 1.0, except at $t = 0$. Therefore S_t is always less than C_{v_t}, except when

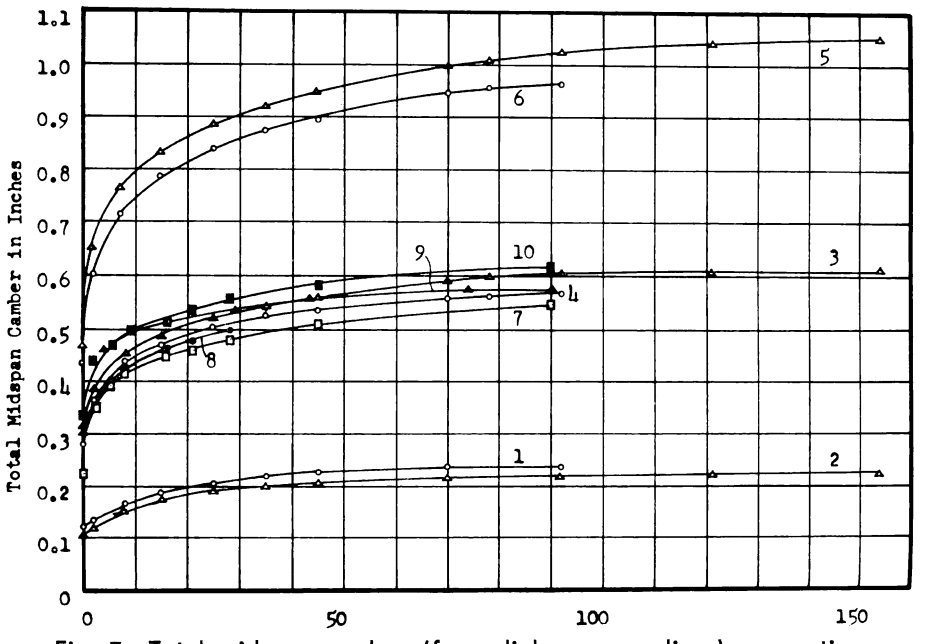

Fig. 7—Total midspan camber (from dial gage readings) versus time

both are zero. Also the first summation term in Eq. (6) is the elastic deflection resulting from the loss of prestress which further reduces S_t.

A second (more direct but less general) approach to the solution of camber deformation in prestressed concrete beams is found by referring to Eq. (2), in which the prestress force was assumed to be constant. The solution of this equation is

$$y = (1 + C_t) \int\int \frac{M_x - P_i e_x}{E_p I} \, dx \, dx$$
$$= (1 + C_t) \, y_i$$

where y_i is the computed initial elastic camber. It is apparent then that the creep coefficient is actually a camber coefficient B_t, which is defined at the ratio of inelastic camber to elastic camber. Hence

$$y = (1 + B_t) \, y_i \qquad (9)$$

or in basic form

$$\frac{d^2y}{dx^2} = \frac{1 + B_t}{E_p I} (M_x - P_i e_x) \qquad (10)$$

Since the theoretical solution given by Eq. (5) requires experimentally determined time-dependent data, this coefficient B_t could be found and used more readily with Eq. (10). The camber coefficient

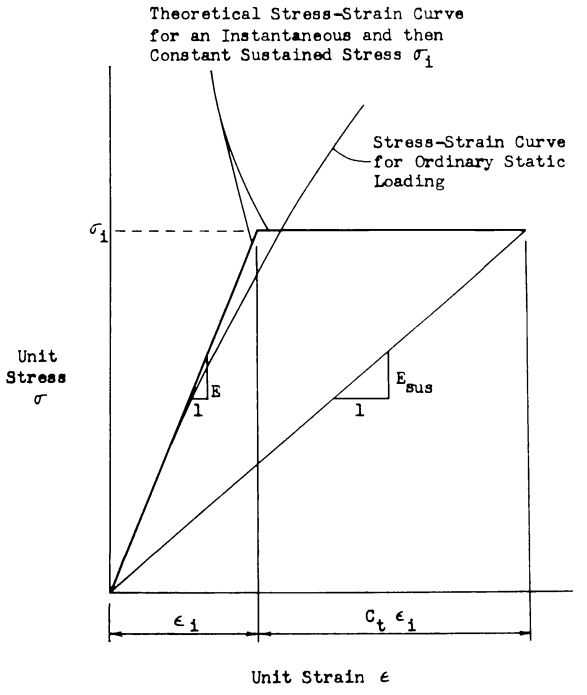

Fig. 8 — Idealized concrete stress-strain curve

B_t is seen to be primarily a property of the concrete (resulting from creep) but includes the effect of prestress loss as well. It would therefore be expected to be smaller than the corresponding creep coefficient as the curves for the two coefficients C_{v_t} (Fig. 9) and B_t (Fig. 12) verify.

The basic camber equation, Eq. (5), which includes Eq. (6) for the coefficient S_t, provides an explanation for the principal factors that affect camber, but these equations are not practical for design purposes covering wide ranges of conditions. However, with the data included herein for the coefficient S_t, the camber deformation can be deter-

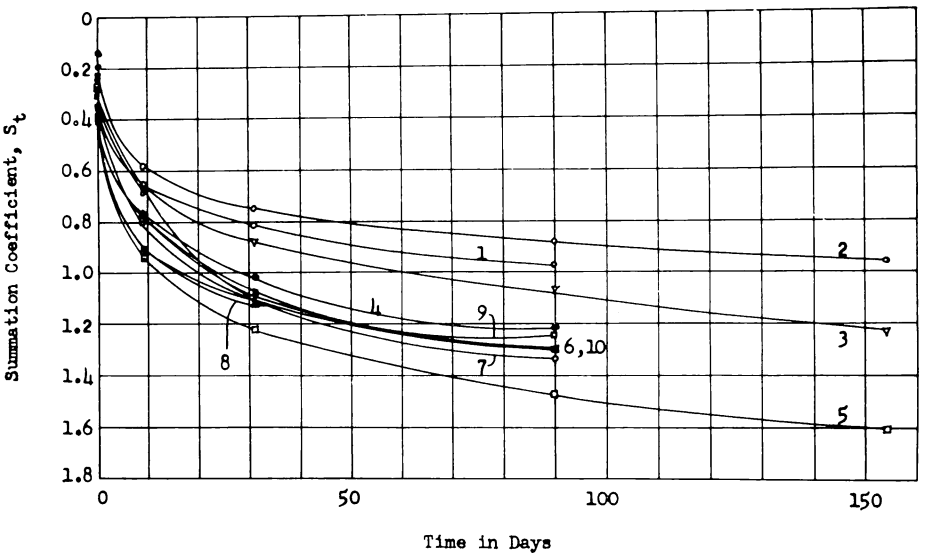

Fig. 9—Creep coefficient under variable sustained stress, C_{v_t} versus time

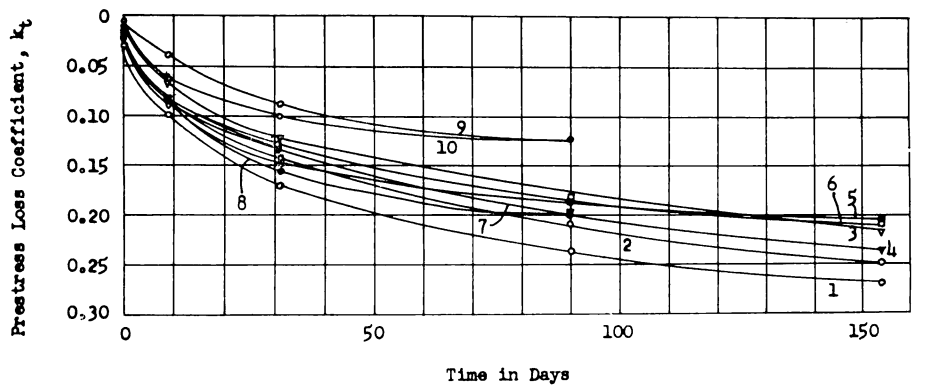

Fig. 10—Prestress loss coefficient, k_t versus time

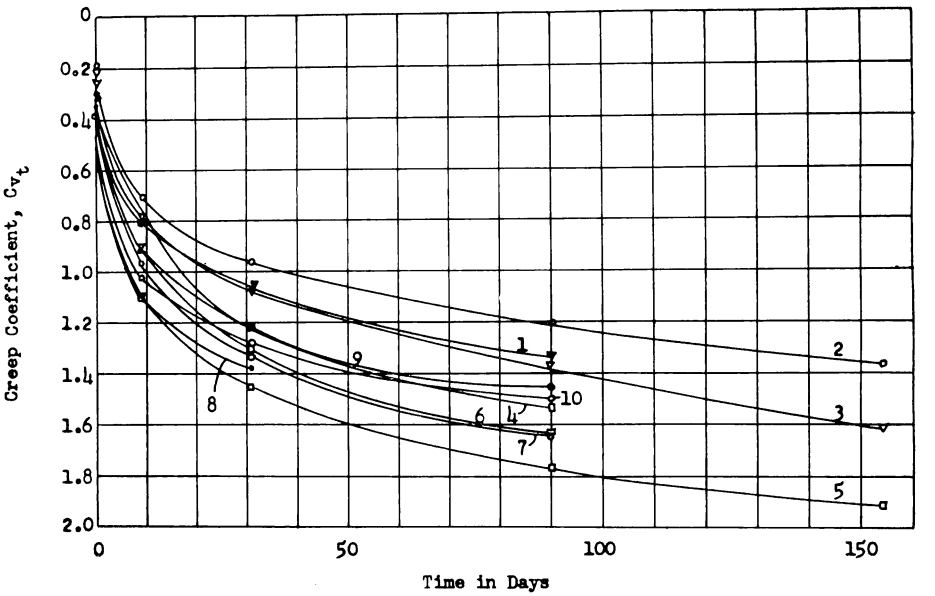

Fig. 11—Summation coefficient, S_t versus time

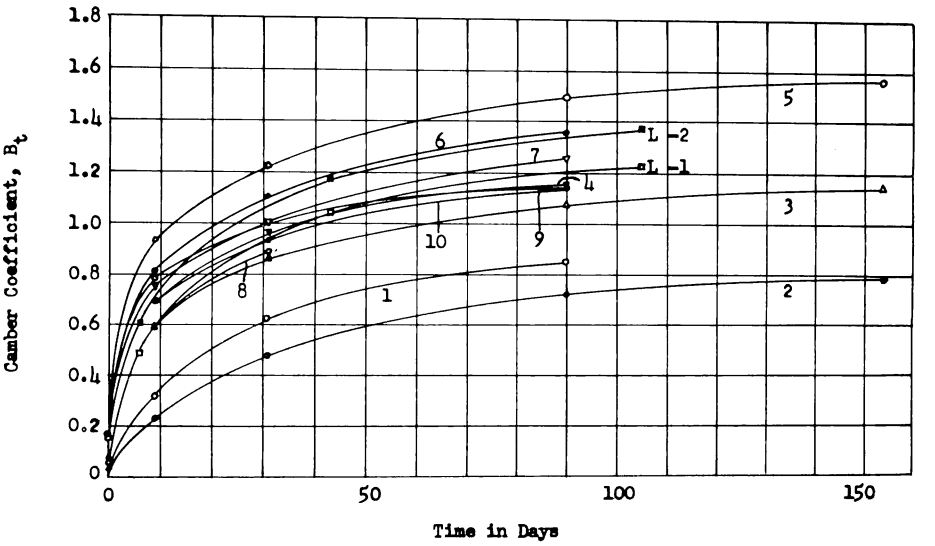

Fig. 12—Camber coefficient, B_t versus time

mined easily with Eq. (7) or (8) for the conditions of these tests. The values for S_t were found to be somewhat less than the creep coefficients C_{v_t} of the corresponding beams, since S_t includes the effects of loss of prestress (see Fig. 9 and 11).

Eq. (10) provides a direct solution to the camber problem using the camber coefficient B_t, which also includes the effect of prestress loss. The values for B_t (Fig. 12) were found to be smaller than the corresponding creep coefficients C_{v_t}.

CAMBER OF COMPOSITE BEAMS

Consider first the case of any sustained load applied to a prestressed concrete beam sometime after prestressing. The strain distribution would be altered, thus requiring a modification of the equations developed in the previous section. Eq. (5) would become

$$\frac{d^2y}{dx^2} = \frac{1}{E_p I}[\,(1 + C_{v_t})\,(M_x) - (1 + S_t)\,(P_i e_x)\,] + \frac{1 + C_{v_{t'}}}{E_q I}\,(M_x') \quad (11)$$

where $C_{v_{t'}}$ is the appropriate creep coefficient for the concrete subjected to sustained stress at the age the additional load was applied, E_q is Young's modulus for the concrete at the age the load was applied, and M_x' is the moment caused by the additional sustained load. Previous observations showed that the creep of concrete is less for sustained loads applied at increasing ages, and hence the creep coefficient $C_{v_{t'}}$ varies depending on the age at which the additional sustained load was applied.

Now consider the special but more practical case of the cast-in-place slab placed to form a composite beam at some date after prestressing. Eq. (11) would apply if the slab were not bonded to the prestressed beam. But since it is, the slab will provide resistance to camber deformation in addition to inducing a downward deflection as a result of the dead load and differential shrinkage.

In considering the strains resulting from creep and differential shrinkage, it is seen that these strains are caused by internal effects and not by any external moment. Hence the composite or transformed section properties are not effective in resisting these strains as a unit. For example, if the stress were zero at the top of the stem of the composite beam, there would be no tendency for the slab to shorten directly as a result of creep in the prestressed stem. The only resistance to camber that it would have would be a bending resistance depending only on the slab *EI* value. The stem *EI* value is a part of the initial strain expression already included. This same concept of separate and not composite resistance also enters into the differential shrinkage theory.

All but the last term of Eq. (11), on the right hand side, is the slope of the elastic-plus-creep strain distribution diagram at the time t, caused by the loading that existed at the time of prestressing. The last term is the decrease in this slope as a result of the additional loading.

Since the problem in the composite beam is to determine the total camber occurring before and after slab casting, Eq. (11) must be modified to include the slab resistance to further bending as a result of creep in the prestressed stem as well as differential shrinkage. This resistance is brought about through a decrease in the creep strains that would occur if there were no bond between the stem and slab. If the differential shrinkage effect is temporarily neglected, the expression for curvature corresponding to the total camber for a composite beam would be

$$\frac{d^2y}{dx^2} = \left[\frac{1}{E_p I_2}(1 + C_{v_q})\,(M_x) - \frac{1}{E_p I_2}\,(1 + S_q)\,(P_i\, e_x) + \frac{1}{E_q I_2}\,(M_x')\right]$$

$$+\left[\frac{C'_{v_{t'}}}{E_p I_2}\,(M_x) - \frac{S'_{t'}}{E_p I_2}\,(P_i\, e_x) + \frac{C_{v_{t'}}}{E_q I_2}\,(M_x')\right]\left[\frac{E_2 I_2}{E_1 I_1 + E_2 I_2}\right] \quad \text{.....(12)}$$

where $C'_{v_{t'}}$ and $S'_{t'}$ are the increase in the coefficients for the time t', but where the sustained stress was applied at the time of prestressing, and q is the time of slab casting. That is,

$$C_{v_t} = C_{v_q} + C'_{v_{t'}} \quad \text{and} \quad S_t = S_q + S'_{t'}$$

The last bracket of Eq. (12) includes the effect of slab resistance since the EI values are the resistance factors for bending. The sum of E_1I_1 and E_2I_2 is used here rather than the EI of the transformed composite section because the continued camber (or deflection) resulting from creep in the precast stem is not resisted by the composite section as a unit. But the two Young's moduli, E_1 and E_2, for the slab and stem, respectively, are increasing with time. However, these two moduli appear in ratio form in the last bracket of Eq. (12) so that the use of the 28-day cylinder moduli for both E_1 and E_2 is sufficient here.

When I_1 becomes zero (no slab), Eq. (12) reduces to Eq. (11). When I_1 increases without bound, but M_x' is finite (deep cast-in-place element), Eq. (12) would show no increase in camber beyond that which occurred up to and immediately following slab casting since the slab dead load factor is in the first bracket to account for this deflection.

The additional decrease in curvature (camber) after the slab has been cast, as a result of the differential shrinkage force F, is given by the expression*

*This was presented more fully in the discussion by the authors of "Differential Shrinkage in Composite Beams," by Halvard W. Birkeland, ACI JOURNAL, V. 32, No. 6, Part 2, Dec. 1960 (*Proceedings* V. 56), pp. 1529-1546.

$$\left[\frac{1 + C_{v_{t'}}}{E_q I_2}\,(g F c_{2T})\right]\left[\frac{E_2 I_2}{E_1 I_1 + E_2 I_2}\right]$$

where g is a factor, less than 1.0, to account for the fact that the total force F does not act over the entire time t'. The force F may be assumed here to remain constant over the entire length of the beam although this is not quite correct.

Because of the general parabolic variation of the differential shrinkage force with time, g is assumed to be 2/3. Hence, including the effect of differential shrinkage, Eq. (12) becomes

$$\frac{d^2y}{dx^2} = \left[\frac{1}{E_p I_2}(1 + C_{v_q})\,(M_x) - \frac{1}{E_p I_2}(1 + S_q)\,(P_i e_x) + \frac{1}{E_q I_2}\,(M_x')\right]$$

$$+\left[\frac{C'_{v_{t'}}}{E_p I_2}\,(M_x) - \frac{S'_{t'}}{E_p I_2}\,(P_i e_x) + \frac{C_{v_{t'}}}{E_q I_2}\,(M_x') + \frac{1 + C_{v_{t'}}}{E_q I_2}\,(\tfrac{2}{3} F c_{2T})\right]$$

$$\left[\frac{E_2 I_2}{E_1 I_1 + E_2 I_2}\right] \qquad (13)$$

It follows that Eq. (10) for the composite beam would become

$$\frac{d^2y}{dx^2} = \left[\frac{1 + B_q}{E_p I_2}\,(M_x - P_i e_x) + \frac{1}{E_q I_2}\,(M_x')\right]$$

$$+\left[\frac{B'_{t'}}{E_p I_2}\,(M_x - P_i e_x) + \frac{B_{t'}}{E_q I_2}\,(M_x') + \frac{1 + B_{t'}}{E_q I_2}\,(\tfrac{2}{3} F c_{2T})\right]$$

$$\left[\frac{E_2 I_2}{E_1 I_1 + E_2 I_2}\right] \qquad (14)$$

Eq. (13) and (14) are also applicable when the precast beam is either symmetrical or unsymmetrical with respect to the horizontal centroidal axis.

The solutions for Eq. (13) and (14) are, respectively,

$$y = \left[\frac{1}{E_p I_2}(1 + S_q)\frac{P_i L^2}{48}\,(e_o + 5e_m) - \frac{1}{E_p I_2}(1 + C_{v_q})\,5wL^4/384\right.$$

$$\left. - \frac{1}{E_q I_2}\,5w'L^4/384\right] + \left[\frac{S'_{t'}}{E_p I_2}\,\frac{P_i L^2}{48}\,(e_o + 5e_m) - \frac{C'_{v_{t'}}}{E_p I_2}\,5wL^4/384\right.$$

$$\left. - \frac{C_{v_{t'}}}{E_q I_2}\,5w'L^4/384 - \frac{1 + C_{v_{t'}}}{E_q I_2}\,\tfrac{2}{3} F c_{2T}\,\frac{L^2}{8}\right]\left[\frac{E_2 I_2}{E_1 I_1 + E_2 I_2}\right] \qquad (15)^*$$

*See Table 4 for an explanation of the terms of Eq. (15).

and

$$y = \left[\frac{1 + B_q}{E_p I_2}\,\frac{P_i L^2}{48}\,(e_o + 5e_m) - \frac{1 + B_q}{E_p I_2}\,5wL^4/384 - \frac{1}{E_q I_2}\,5w'L^4/384\right]$$

$$+\left[\frac{B'_{t'}}{E_p I_2}\,\frac{P_i L^2}{48}\,(e_o + 5e_m) - \frac{B'_{t'}}{E_p I_2}\,5wL^4/384 - \frac{B_{t'}}{E_q I_2}\,5w'L^4/384\right.$$

$$\left. - \frac{1 + B_{t'}}{E_q I_2}\,\tfrac{2}{3}\,F\,c_{2T}\,\frac{L^2}{8}\right]\left[\frac{E_2 I_2}{E_1 I_1 + E_2 I_2}\right] \qquad (16)$$

Both of these equations provide the solution for midspan camber of composite beams. Eq. (15) involves the use of the summation coefficient S and the creep coefficient C_v while Eq. (16) includes the camber coefficient B.

EXPERIMENTALLY DETERMINED COEFFICIENTS

The values of the creep coefficient C_{v_t} were determined from the strain distribution diagrams for the total measured-strain-less-shrinkage strain. The strains at the bottom fiber were used. Only the average of the end and midspan values are reported since these were practically the same. The elastic strain resulting from loss of prestress was discounted to obtain the true creep coefficient. The actual values for the creep coefficient were based on the computed initial elastic strain. This was found to be necessary to correlate all of the theoretical and experimental camber data. The values for the creep coefficient C_{v_t} versus time are shown in Fig. 9 for the test beams.

The loss of prestress was determined from the concrete shrinkage-plus-creep strains (at the beam ends) at the level of each bar using the strain distribution diagrams, and also from direct strain readings on the bars themselves using electrical gages. There was reasonably close agreement between the two methods. The precentage loss of prestress (in decimal form as the prestress loss coefficient k_t) versus time curves are shown in Fig. 10, for which an average of the three bars were used for each beam.

The effect of prestress loss on camber can best be described by referring to the summation coefficient S_t, which was defined by Eq. (6). The first term is the elastic deflection resulting from the loss of prestress, and the second term is the creep effect with the variable prestress force given by $(1 - k_t)\,P_i$ for any time t. Hence the summation coefficient S_t, involving the time-dependent variables of percentage prestress loss k_t, concrete stiffness $E_{t'}$ and the creep coefficient $C_{v_{t'}}$, corresponds to the creep coefficient for the constant sustained moment M_x. It therefore includes the total time-dependent effect on camber for

the prestress moment $P_i e_x$. It is seen from the curves in Fig. 11 that each coefficient S_t has approximately the same relative position as the corresponding creep coefficient C_{v_t} (Fig. 9), but the S_t values are smaller in every case because of the effect of prestress loss.

The camber coefficient B_t was defined as the ratio of inelastic camber to elastic camber. The values for the camber coefficient were determined by dividing the total measured camber minus the initial theoretical elastic camber (using the cylinder value for Young's modulus) by the elastic camber. It is seen by Eq. (9) that this coefficient corresponds to the creep coefficient. Hence the time-dependent camber is a direct result of concrete creep. In fact, the camber coefficient and creep coefficient would be equal except that the camber coefficient includes the effect of prestress loss.

The same solution is obtained in camber calculations if the camber coefficient is included in the expression for the sustained modulus. In this case

$$E_{sus} = \frac{E_p}{1 + B_t} \qquad (17)$$

or

$$\frac{E_{sus}}{E_p} = \frac{1}{1 + B_t} \qquad (18)$$

where E_p is the cylinder modulus at the time of prestressing, B_t is the camber coefficient (actually a creep coefficient but including the elastic and inelastic effect of prestress loss), and E_{sus} is the sustained modulus to be used for any time t to determine the total camber. The values for the camber coefficient B_t versus time are shown in Fig. 12 and for E_{sus}/E_p versus time in Fig. 13 for the test beams.

DISCUSSION OF RESULTS

The experimental data included in the camber investigation provided an insight into the nature of initial-plus-time-dependent camber deformation. The midspan camber for each beam was measured directly using dial gages for the noncomposite beams and a level for the composite beams. Measured strains were also used in the camber study.

The equations previously developed for solving the camber problem involved, in every case, an experimentally determined coefficient which was primarily a function of concrete creep. These coefficients (C_{v_t}, S_t, B_t, and E_{sus}) were evaluated for the test beams and are shown in Fig. 9, 11, 12, and 13, respectively. The prestress loss coefficient (k_t) was evaluated for each beam and is presented in Fig. 10.

Each of these five sets of curves provide a means of studying the effects of the variables considered in the test beams. The variables

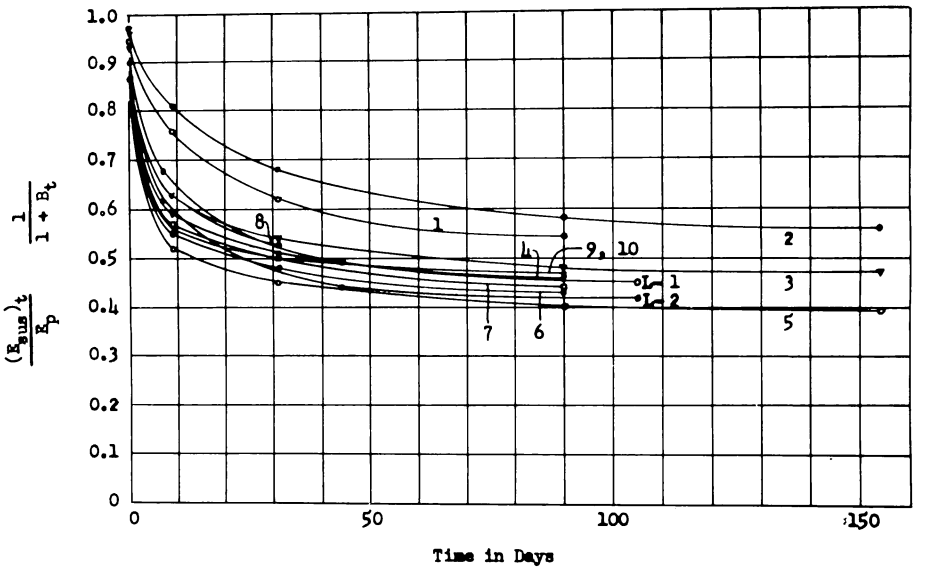

For Beams 1-6, $E_p = 4.25 \times 10^6$ psi
For Beams 7-10, $E_p = 4.01 \times 10^6$ psi
For Beams L-1 and L-2, $E_p = 4.50 \times 10^6$ psi

Fig. 13—Ratio of sustained modulus, E_{sus} to cylinder modulus at time of prestressing, E_p versus time

included in the camber study were prestress level, concrete strength, and surrounding atmospheric conditions (principally relative humidity). A summary of the testing conditions and variables considered are shown in Table 3, along with the numerical values for the different coefficients at 90 days following prestressing.

By comparing Beams 1,2; 3,4; and 5,6; the creep coefficient C_{v_t} in the prestressed concrete beam is seen to vary in slightly increasing proportion with magnitude of the prestress force. The effect of the 72 and 90 percent average relative humidities (Beams 7 and 9,10) caused a difference of about 9 percent (1.64 and 1.48, respectively) in the creep coefficient. As would be expected, the value is higher in the lower humidity region. By comparing Beams 3,4; 5,6; and 7; the creep coefficient is seen to vary more closely with prestress level (relative to concrete strength) than to just prestress magnitude itself for different concrete strengths. A comparison of Beams 3,4, and 7 shows the creep coefficient to be about 12 percent greater (1.64 and 1.45) for the weaker concrete under the same prestress force.

The percentage prestress loss varied from 22.4 percent to 18.3 percent for the different prestress levels. The smaller prestress level (Beams 1 and 2) showed the largest percentage of loss in prestress. The reason for this is that the effect of creep on prestress loss is approximately

proportional to stress level, but the effect of concrete shrinkage on prestress loss is independent of prestress level. Hence the lower initial prestress force would have the higher percentage loss. The effect of the 72 and 90 percent average relative humidities (Beams 7 and 9,10, respectively) caused a big difference (20.1 and 12.4 percent, repectively) in the prestress loss percentage. The principal reason for this is the greater concrete shrinkage in the lower humidity region, although the effect of concrete creep also contributed somewhat to this difference. By comparing Beams 3,4, and 7, it is seen that the percentage of prestress loss was less in the stronger concrete beams (18.3 and 20.1 percent, respectively). The reason for this was the smaller creep strain in the stronger concrete since the shrinkage strain was about the same for both.

The same comparisons that were made for the creep coefficient C_{v_t} are seen in Table 3 to closely apply to the summation coefficient S_t and the camber coefficient B_t, since these coefficients were essentially creep coefficients that included the effects of prestress loss in the prestressed concrete beams. However, the camber coefficient B_t and the corresponding sustained modulus E_{sus} ($E_{sus} = E_p/1 + B_t$) are direct func-

TABLE 3 — SUMMARY OF TESTING CONDITIONS AND EFFECTS OF VARIABLES IN CAMBER STUDY

Beam No.	Concrete strength 28 days, psi	Stress level percent f'_{ci}	psi	Location	Average relative humidity, percent	Concrete age when prestressed, days
1,2	5030	25	1250	Lab	77	28
3,4	5030	45	2250	Lab	77	28
5,6	5030	65	3250	Lab	77	28
7,8	3760	60	2250	Lab	72	28
9,10	3760	60	2250	Field	90	28

Experimental values at 90 days following prestressing

Prestress level

Beam No.	C_{v_t}	k_t	S_t	B_t	$\frac{E_{sus}}{E_p}$	E_{sus}†
1,2*	1.28	0.224	0.93	0.79	0.56	2.38
3,4	1.45	0.183	1.15	1.11	0.47	2.00
5,6	1.70	0.184	1.39	1.42	0.42	1.78

Relative humidity

7	1.64	0.201	1.33	1.25	0.44	1.77
9,10	1.48	0.124	1.28	1.14	0.47	1.89

Concrete strength

3,4	1.45	0.183	1.15	1.11	0.47	2.00
5,6	1.70	0.184	1.39	1.42	0.42	1.78
7	1.64	0.201	1.33	1.25	0.44	1.77

*Average values were used for the beam pairs except for Beam 8 which was used to form a composite beam at 37 days following prestressing.

†The sustained modulus E_{sus} is in psi $\times 10^6$. The other coefficients are dimensionless quantities.

tions of the initial-plus-time-dependent camber deformation and the effects of the three variables considered on these values are a direct indication of their effects on total camber. The camber coefficient is the percentage increase in camber above the computed initial camber (in decimal form) using the cylinder value for Young's modulus at the time of prestressing, E_p.

The sustained modulus E_{sus} includes the effects of both concrete creep and prestress loss. The values of E_{sus}/E_p (0.56, 0.47, and 0.42) for Beams 1,2; 3,4; and 5,6, respectively, show the effect of prestress level on the sustained modulus. It is seen that the lowest prestress level beam has an increasingly higher value because of the greater percentage prestress loss. The effect of the 72 and 90 percent average relative humidities (Beams 7 and 9,10, respectively) caused a difference of about 7 percent (0.44 and 0.47, respectively) in the values of E_{sus}/E_p and thus a difference in the values of the total camber deformation. The lower humidity region had the lower sustained modulus value and the larger total camber as would be expected.

By comparing Beams 3,4; 5,6; and 9,10 (E_{sus}/E_p = 0.47, 0.42, 0.44, and 0.47 or E_{sus} = 2.00, 1.78, 1.77, and 1.89 $\times$ 10^6, respectively), it is considered significant that the total camber was noticeably insensitive to the effects of relative humidity and concrete strength. The reason for this is that there is a tendency for the effect of greater creep and resulting greater camber growth to be offset by a greater loss of prestress caused by both shrinkage and creep and the resulting reduction in camber growth. The maximum difference in the total camber (as reflected in the E_{sus}/E_p values) was about 11 percent. This was true even for Beams L-1 and L-2 of Lofroos and Ozell[2] (E_{sus}/E_p = 0.44 and E_{sus} = 1.98 $\times$ 10^6) which were 5 ft longer and 2 in. wider than the other beams tested.

Troxell[3] determined that the shrinkage and creep of concrete at 90 days are about 60 percent of their ultimate values. Based on this percentage, the ultimate value for the creep coefficient C_{v_t} is 2.3 for the usual prestress levels. This was found to vary only slightly between the laboratory and field conditions of these tests and the different concrete strengths used. The ultimate percentage of prestress loss was found to be about 30 percent for the laboratory conditions and about 20 percent for the field conditions. These values are considerably higher than those used in current design practice (about 15 percent for post-tensioned beams). One reason for using this lower value may be that concrete strength also increases with age. However, for Type I cement, the concrete strength at 90 days is approximately 90 percent of its ultimate value. Hence it is believed that higher values for the percentage of prestress loss than the ordinary rule of thumb value of 15 percent for post-tensioned beams are in order. The methods used

for this part of the experimental investigation were substantiated by two independent types of measurements.

The summation coefficient S_t, the camber coefficient B_t, and the sustained modulus E_{sus} do not follow the same time-dependent increase for long periods. As the curves in Fig. 11, 12, and 13 indicate, the ultimate values appear to have been nearly reached at the end of the test period. The curves for the creep coefficient C_{v_t} (Fig. 9) and the prestress loss coefficient k_t (Fig. 10) are seen to be decidedly steeper or continuing to increase more at the end of the test period. The reason for this will now be discussed in relation to the ultimate camber deformation in prestressed concrete beams.

There is little doubt that concrete shrinkage and creep continue appreciably for long periods. However, the total camber deformation (determined by the sustained modulus) is primarily a function of creep only, since the sustained modulus for a constant sustained stress is given by

$$E_{sus} = \frac{E_c}{1 + C}$$

where C is the creep coefficient. But in the case of the prestressed concrete beam, the sustained prestress force is not constant, and concrete creep also tends to reduce camber growth through its effect on the loss of prestress. In addition, concrete shrinkage has the main function of reducing the camber growth through its effect on the loss of prestress.

It appears evident, therefore, that the camber growth would tend to reach a maximum value relatively early compared to the long-time shrinkage and creep strains that would be expected. In fact, there may even begin to be a reduction in camber or downward deflection after a few hundred days. This would be brought about through the continued loss of prestress resulting from both shrinkage and creep plus any effect that time may have on increasing the frictional force

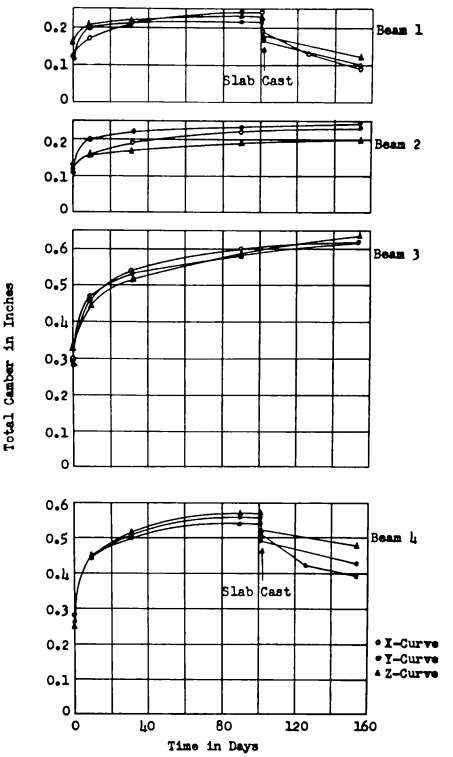

Fig. 14—Comparison of midspan camber by three methods (Beams 1-4)

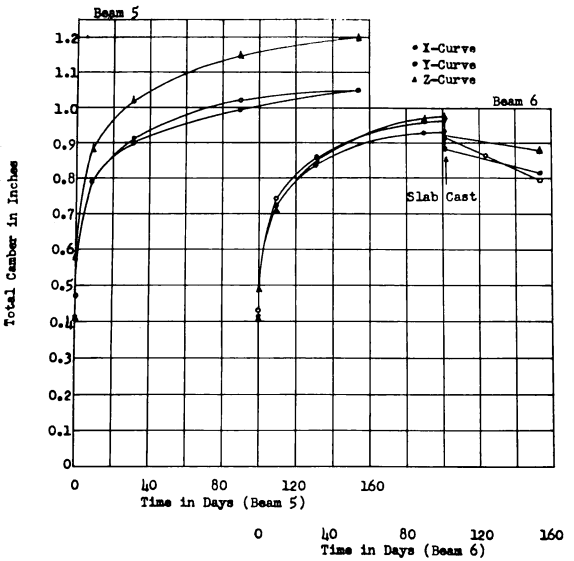

Fig. 15—Comparison of midspan camber by three methods (Beams 5 and 6)

at the roller end. For camber growth to continue freely, the two ends of the beam at the bottom must necessarily be permitted to decrease their distance between each other. The measured camber curves in Fig. 7 show that the total camber for the test beams seem to reach their maximum values from about 100 to 200 days depending on the prestress level.

For ordinary prestress levels, the ultimate values for the respective coefficients appear to be $S_u = 1.4$, $B_u = 1.2$, and $E_{sus}/E_p = 0.45$. The value for the corresponding ultimate sustained modulus to be used in camber calculations is $E_{sus} = 1.9 \times 10^6$ psi. These values were found to vary only slightly between the different concrete strengths and relative humidities of this investigation. It was also found for ordinary prestress levels that the camber increased about 10 percent above the computed initial camber during the first ½ hr, about 30 percent during the first 24 hr, and about 110 percent after 90 days following prestressing. These figures correspond to sustained moduli of $E_p/1.10$, $E_p/1.30$, and $E_p/2.10$, respectively, where E_p is the cylinder value for Young's modulus at the time of prestressing.

The midspan camber for each beam was determined in three independent ways and compared in Fig. 14-16. The three different methods referred to as X, Y, and Z are described as follows:

X—Camber from direct measurement using dial gages for the noncomposite beams and level readings for the composite-beam portion of the curves. This is exactly the same as the camber that could be computed using the camber coefficient B_t or the sustained modulus E_{sus} since these factors were determined from the measured camber.

Y—Computed camber using the basic camber equation involving the summation coefficient S_t (Eq. (8) for the noncomposite beams and Eq. (15) for the composite beams). The parabolic cable solution was necessary because of the displacement of the unbonded bars relative to the centroidal axis during the camber deformation. The bar eccentricities and prestress forces were determined by measurement.

Z—Camber computed by Eq. (20) using the slope of the strain distribution diagrams drawn from the total measured strain less shrinkage strain. A sample of these diagrams is shown in Fig. 6. This was used simply as a third independent determination of the total camber for comparison purposes.

The time-dependent curvature expression for a beam which is bending is given by the expression

$$\frac{d^2y}{dx^2} = -H_x \quad \text{.....(19)}$$

where H_x is the slope of the elastic-plus-creep strain distribution diagram $(\varepsilon/d)_x$ as a function of x. For a parabolic variation of H_x, the midspan camber solution becomes

$$y = (H_{end} + 5\,H_{mid})\,L^2/48 \quad \text{.....(20)}$$

This equation is used in connection with Method Z for calculating camber.

The camber curves in Fig. 14 through 16 were determined for each beam by the three methods X, Y, and Z. The three curves for each beam were found to be in reasonably close agreement, which substantiates the experimental data and the formulas presented for computing camber deformation.

An understanding of the relative influences of the different factors affecting the total camber of composite beams can be obtained by referring to Table 4, which gives an explanation and solution for each term of Eq. (15). There is thought to be no short method for calculating the time-dependent camber in composite beams, since several factors

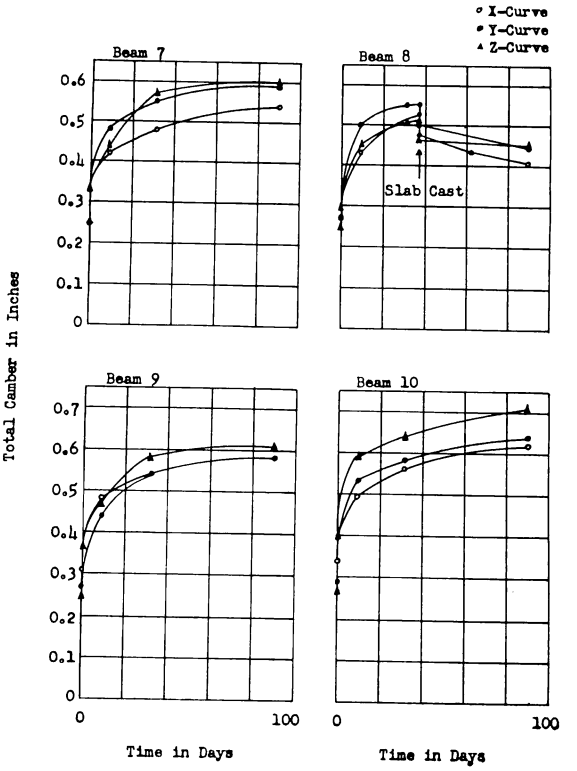

Fig. 16—Comparison of midspan camber by three methods (Beams 7-10)

TABLE 4 — CAMBER SOLUTION FOR COMPOSITE BEAMS

$$y = \left[\underbrace{\frac{1}{E_p I_2}(1 + S_q)\frac{P_i L^2}{48}(e_o + 5e_m)}_{(1)} - \underbrace{\frac{1}{E_p I_2}(1 + C_{v_t}\frac{5wL^4}{384}}_{(2)} - \underbrace{\frac{1}{E_q I_2}\frac{5w'L^4}{384}}_{(3)}\right]^*$$

$$+\left[\underbrace{\frac{S'_{t'}}{E_p I_2}\frac{P_i L^2}{48}(e_o + 5e_m)}_{(4)} - \underbrace{\frac{C'_{v_{t'}}}{E_p I_2}\frac{5wL^4}{384}}_{(5)} - \underbrace{\frac{C_{v_{t'}}}{E_q I_2}\frac{5w'L^4}{384}}_{(6)}\right.$$

$$\left.\underbrace{-\frac{1 + C_{v_{t'}}}{E_q I_2}\tfrac{2}{3}F c_{2T}\frac{L^2}{8}}_{(7)}\right]^\dagger \underbrace{\left[\frac{E_2 I_2}{E_1 I_1 + E_2 I_2}\right]}_{(8)} \qquad (15)$$

(1) Elastic-plus-inelastic camber resulting from the prestress force up to the time of slab casting $t = q$

(2) Elastic-plus-inelastic deflection resulting from the precast beam dead load up to the time of slab casting

(3) Elastic deflection resulting from slab dead load

(4) Inelastic camber resulting from the prestress force after the slab was cast or time t' (Note $S_t = S_q + S'_{t'}$ or $S'_{t'} = S_t - S_q$)

(5) Inelastic deflection resulting from the precast beam dead load after the slab was cast (Note $C_{v_t} = C_{v_q} + C'_{v_{t'}}$ or $C'_{v_{t'}} = C_{v_t} - C_{v_q}$)‡

(6) Inelastic deflection resulting from the slab dead load

(7) Total deflection resulting from differential shrinkage

(8) Factor which includes the slab resistance to bending

Beam No.	(1)	(2)	(3)	(4)	(5)	(6)	(7)	(8)
1-C	0.392	−0.168	−0.050	0.012	−0.008	−0.036	−0.049	0.950
4-C	0.721	−0.179	−0.050	0.036	−0.013	−0.041	−0.049	0.950
6-C	1.112	−0.185	−0.050	0.048	−0.008	−0.045	−0.049	0.950
8-C	0.738	−0.177	−0.054	0.058	−0.018	−0.060	−0.051	0.948

Beam No.	[(1)+(2)+(3)] = (9)	[(4)+(5)+(6)+(7)](8) = (10)	y = (9)+(10), in.	Time, t, days
1-C	0.176	−0.077	0.099	154
4-C	0.492	−0.064	0.428	154
6-C	0.877	−0.051	0.826	154
8-C	0.507	−0.067	0.440	90

*Total camber immediately after slab casting = [(1) + (2) + (3)] = (9)

†Total camber or deflection for time t' which is the time measured from the day of slab casting = [(4) + (5) + (6) + (7)](8) = (10)

‡Note that the $C_{v_{t'}}$ values were determined as follows:

Beams 1-C, 4-C, and 6-C; 60 percent and for Beam 8-C; 80 percent of the corresponding values when loaded at 28 days were used.

must be considered, as indicated by Eq. (15). This equation is helpful in understanding the relative importance of the different factors and could be used without too much difficulty in design. The values for the differential shrinkage force F used in the solutions shown in Table 4 were taken from Reference 11.

CONCLUSIONS

The following conclusions are drawn concerning the time-dependent effects in both noncomposite and composite post-tensioned concrete members:

1. For design purposes, the total (initial-plus-time-dependent) camber deformation for noncomposite beams is readily obtained by Eq. (10) using either the camber coefficient B_t or the sustained modulus E_{sus}. However, the basic camber equation developed herein, Eq. (5), is required for a more rational analysis of noncomposite beam camber. The rational analysis of composite beam camber requires the solution of Eq. (15) or (16). These two equations are not practical for design purposes. However, any simpler method is not recommended since it would require the use of approximations that may lead to erroneous results.

2. Camber deformation for ordinary prestress levels ($0.45 f'_{ci}$) increases about 10 percent above the computed initial camber (using the cylinder modulus of elasticity) during the first ½ hr, about 30 percent during the first 24 hr, and about 110 percent during the first 90 days following prestressing.

3. Total camber deformation is noticeably insensitive to the effects of relative humidity and concrete strength, because there is a tendency for greater time-dependent concrete strains resulting from creep and shrinkage to be offset by greater losses of prestress. The maximum difference in the total camber of the test beams was about 11 percent for these two variables.

4. Total camber deformation appears to be more closely related to the prestress level (relative to concrete strength) than to the actual prestress magnitude itself.

5. Total camber deformation may reach its ultimate value relatively early (100 to 200 days) compared to the long-time shrinkage and creep strains that would be expected. The following ultimate values are recommended for ordinary prestress levels in post-tensioned members: the prestress loss percentage of 20 percent for average relative humidity of about 90 percent and 30 percent for average relative humidity of about 70 percent, the creep coefficient $C_{v_u} = 2.3$, the summation coefficient $S_u = 1.4$, the camber coefficient $B_u = 1.2$, and the sustained modulus $E_{sus}/E_p = 0.45$ or $E_{sus} = 1.9 \times 10^6$ psi. These values for C_{v_u}, S_u,

B_u, E_{sus}/E_p, and E_{sus} are subject to some variation for different concrete strengths and relative humidities, but it is believed that for high-strength concrete the variation would be relatively small.

ACKNOWLEDGMENTS

The authors wish to express their appreciation to the Florida State Road Department for sponsoring the research program of which this investigation was a part. Acknowledgment is also made to Stressteel Corp. and Flexico Products, Inc. for the donation of the post-tensioning bars and flexible tubing used in the preparation of the test specimens.

REFERENCES

1. ACI-ASCE Committee 327, "Report of ASCE-ACI Joint Committee on Ultimate Strength Design," *Proceedings,* ASCE, V. 81, Oct. 1955, Paper No. 809. "Ultimate Strength Design," ACI JOURNAL, V. 27, No. 5, Jan. 1956 (*Proceedings* V. 52), pp. 505-524.

2. Lofroos, W. N., and Ozell, A. M., "The Apparent Modulus of Elasticity of Prestressed Concrete Beams Under Different Stress Levels," *Journal,* Prestressed Concrete Institute, V. 4, No. 2, Sept. 1959, pp. 23-47.

3. Troxell, G. E.; Raphael, J. M.; and Davis, R. E., "Long Time Creep and Shrinkage Tests of Plain and Reinforced Concrete," *Proceedings,* ASTM, V. 58, 1958, pp. 1-20.

4. Freudenthal, A. M., and Roll, Frederic, "Creep and Creep-Recovery of Concrete Under High Compressive Stress," ACI JOURNAL, V. 29, No. 12, Sept. 1955 (*Proceedings* V. 54), pp. 1111-1142.

5. Ross, A. D., "Creep of Concrete Under Variable Stress," ACI JOURNAL, V. 29, No. 9, Mar. 1958 (*Proceedings* V. 54), pp. 739-758.

6. McCann, Ray A., "Chamber Control," *Journal,* Prestressed Concrete Institute, V. 2, No. 4, Mar. 1958, pp. 75-76.

7. Proceedings of the Fourth Annual Convention, Prestressed Concrete Institute, Sept. 1958, pp. 33-48.

8. Branson, D. E., and Ozell, A. M., "A Report on Differential Shrinkage in Composite Prestressed Concrete Beams," *Journal,* Prestressed Concrete Institute, V. 4, No. 3, Dec. 1959, pp. 61-79.

9. Magnel, G., *Prestressed Concrete,* 3rd Edition, McGraw-Hill Book Co., New York, 1954, 345 pp.

10. Komendant, A., *Prestressed Concrete Structures,* McGraw-Hill Book Co., New York, 1952, 261 pp.

11. Branson, D. E., "Time Dependent Effects in Non-Composite and Composite Prestressed Concrete Beams," PhD Thesis, University of Florida, Gainesville, 1960.

Received by the Institute Sept. 12, 1960. Title No. 57-68 is a part of copyrighted Journal of the American Concrete Institute, V. 32, No. 12, June 1961 (Proceedings V. 57). Separate prints are available at 60 cents each.

American Concrete Institute, P. O. Box 4754, Redford Station, Detroit 19, Mich.

Discussion of this paper should reach ACI headquarters in triplicate by Sept. 1, 1961, for publication in Part 2, December 1961 JOURNAL.